Phys. Proc. Ultra-Peripheral Collisions **2**, 007 (2026) 1-7

Momentum transfer dependence in electronuclear production of heavy quarkonia revisited: Green's function formalism

J. Óbertová[1 a] and J. Nemchik[1,2 b]
[1] *Czech Technical University in Prague, FNSPE, Břehová 7, 11519 Prague, Czech Republic*
[2] *Institute of Experimental Physics SAS, Watsonova 47, 04001 Košice, Slovakia*

Momentum transfer distributions $d\sigma/dt$ in diffractive electroproduction of heavy quarkonia on nuclear targets are studied within a rigorous quantum-mechanical approach based on the light-front Green's function formalism. Such a formalism allows to include naturally the higher-twist and leading-twist shadowing corrections, as well as the color transparency effects. Model calculations of $d\sigma/dt$, containing also the correlation between impact parameter of a collision $\vec{b}$ and dipole orientation $\vec{r}$, are tested by the recent data on charmonium production in ultra-peripheral nuclear collisions on proton and lead target. In model predictions on nuclear target, the reduced quark shadowing leads to a significant decrease in $d\sigma/dt$ in kinematic regions scanned by experiments at the prepared electron-ion collider at Brookhaven National Laboratory. At high energies, relevant to current Large-Hadron-Collider and future Large-Hadron-Electron-Collider experiments, the gluon shadowing causes a non-monotonic energy dependence of $d\sigma/dt$ which may indicate possible onset of gluon saturation effects.

DOI: https://doi.org/10.17161/rrcspj62
Keywords: charmonia, momentum transfer, Green's function, shadowing

1 Introduction

Coherent photo- and electroproduction of heavy quarkonia off nuclei represents an effective tool for investigation of the quantum coherence that is related to nuclear shadowing effects. Within a quantum chromodynamics (QCD) color dipole approach, such a process can be described as a result of the photon interaction through its Fock components, $|Q\bar{Q}\rangle$, $|Q\bar{Q}G$, $|Q\bar{Q}2G\rangle$, ... with nuclear targets [1,2]. The contribution of each Fock state to nuclear shadowing is treated separately in accordance with the coherence length (CL) representing its lifetime during propagation through the nuclear medium.

For the $Q\bar{Q}$ photon fluctuation, the corresponding CL reads

$$l_c = \frac{W^2 + Q^2 - m_N^2}{m_N(M_V^2 + Q^2)}\,, \tag{1}$$

where W is the c.m. energy of the photon-nucleon system; m_N and M_V are the masses of the nucleon and vector meson, respectively, and Q^2 is the photon virtuality. The onset of the maximal initial state quark shadowing requires an inequality, $l_c \gg R_A$, where R_A is the nuclear radius.

For higher $|Q\bar{Q}G\rangle$ Fock state the corresponding coherence length has the form

$$l_c^G = \frac{(W^2 + Q^2 - m_N^2)\cdot \alpha_g(1-\alpha_g)}{m_N\Big[k_T^2 + (1-\alpha_g)\,m_g^2 + \alpha_g M_{\bar{Q}Q}^2 + \alpha_g(1-\alpha_g)\,Q^2\Big]}\,, \tag{2}$$

where k_T is the gluon transverse momentum, $M_{\bar{Q}Q}$ is the effective mass of the $\bar{Q}Q$ pair, α_g is the light-front (LF) fraction of the photon momentum carried by the gluon, and the effective gluon mass $m_g \approx 0.7\,\text{GeV}$ [3]. The onset of gluon shadowing (GS) relies on the condition of sufficiently long $l_c^G \gg d$, where $d \approx 2$ fm is the mean separation between bound nucleons. One can also see that $l_c^G \ll l_c$ due to small $\alpha_g \ll 1$ [4]. For higher multi-gluon Fock components of the photon there are strong inequalities, $l_c^{nG} \ll l_c^{(n-1)G} \ll ... \ll l_c^{2G} \ll l_c^G$. This leads to the conclusion that the more gluons are included in the Fock state, the larger photon energy is required for the manifestation of shadowing effects.

We study such shadowing effects in the transverse momentum transfer distributions $d\sigma/dt$ of coherent photo- and electroproduction of charmonia on nuclear targets. Here we analyze the processes in nuclear ultra-peripheral and electron-ion collisions. In particular, the quark and gluon shadowing effects related

[a] Speaker, email: jaroslava.obertova@fjfi.cvut.cz
[b] email: jan.nemcik@fjfi.cvut.cz

to the lowest and higher Fock components of the photon are quantified exploring the energy dependence of t-dependent differential cross sections. The nuclear shadowing is analyzed in the broad energy range. In the kinematic region of the planned Electron-Ion-Collider (EIC) experiment [5] we expect a manifestation of the reduced quark shadowing effect, when the coherence length l_c, Eq. (1), becomes comparable to or smaller than the nuclear radius, $l_c \lesssim R_A$. At sufficiently high energies, relevant for future Large-Hadron-Electron-Collider (LHeC) experiments [6], we study how the effect of gluon shadowing from higher multi-gluon Fock components of the photon affects the transverse momentum distributions. Such a study is relevant for searching for a signal of gluon saturation since the reduction of the gluon distribution function due to GS corresponds to a non-linear QCD evolution incorporated into evolution equations [7,8,9,10].

2 Model

The study is performed within the light-front color dipole approach [11, 12] based on the Green's function formalism [13]. Here, we briefly introduce the formalism, more details regarding the model can be found in Ref. [2]. The amplitude for the electroproduction of heavy quarkonia on a nuclear target, assuming the lowest $|Q\bar{Q}\rangle$ Fock component of the photon, is of the form:

$$\mathcal{A}^{\gamma^* A\to VA}(x,Q^2,\vec{q}) = 2\int d^2b \int d^2b_A\ \exp\Big[\,i\,(\vec{b}+\vec{b}_A)\cdot\vec{q}\,\Big]\int_{-\infty}^{\infty} dz\,\rho_A\big(\vec{b}+\vec{b}_A,z\big)\,F_1(x,Q^2,\vec{q},\vec{b},\vec{b}_A,z)\,. \quad (3)$$

Here, $\vec{b}$ is the impact parameter of the proton-dipole collision, $\vec{b}_A$ is the nuclear impact parameter, $\rho_A(\vec{b},z)$ is the Wood-Saxon nuclear density distribution [14], and $\vec{q}$ is the transverse momentum transfer. The function $F_1(x,Q^2,\vec{q},\vec{b},\vec{b}_A,z)$ is expressed as

$$\begin{aligned} F_1(x,Q^2,\vec{q},\vec{b},\vec{b}_A,z) &= \int_0^1 d\alpha \int d^2r_1\,d^2r_2\,\Psi_V^*(\vec{r}_2,\alpha)\,G_{Q\bar{Q}}(z_2\to\infty,\vec{r}_2;z_1,\vec{r}_1|\vec{b}_A) \\ &\times\ \mathcal{A}^N_{\bar{Q}Q}(\vec{r}_1,x,\alpha,\vec{b})\,\Psi_{\gamma^*}(\vec{r}_1,\alpha,Q^2)\,, \end{aligned} \quad (4)$$

where $\Psi_V(\vec{r_2},\alpha)$ is the LF vector meson wave function obtained by Terent'ev prescription [15] including the Melosh spin rotation effect [16] and $\Psi_{\gamma^*}(\vec{r}_1,\alpha,Q^2)$ is the wave function of the photon. The LF wave functions depend on transverse separation $\vec{r}$ and the fraction of LF momentum α carried by a heavy quark or antiquark. The amplitude $\mathcal{A}^{\gamma^* A\to VA}(x,Q^2,\vec{q})$ depends on Bjorken x defined as

$$x = \frac{M_V^2+Q^2}{s} = \frac{M_V^2+Q^2}{W^2+Q^2-m_N^2}\,. \quad (5)$$

The partial dipole-proton amplitude $\mathcal{A}^N_{\bar{Q}Q}(\vec{r}_1,x,\alpha,\vec{b})$ including $\vec{r}-\vec{b}$ correlation [12] is defined as follows

$$\begin{aligned} \mathrm{Im}\mathcal{A}^N_{\bar{Q}Q}(\vec{r},x,\alpha,\vec{b}\,) = \frac{\sigma_0}{8\pi\mathcal{B}(x)}\Bigg\{&\exp\left[-\frac{\big[\vec{b}+\vec{r}(1-\alpha)\big]^2}{2\mathcal{B}(x)}\right]+\exp\left[-\frac{(\vec{b}-\vec{r}\alpha)^2}{2\mathcal{B}(x)}\right] \\ &-2\,\exp\left[-\frac{r^2}{R_0^2(x)}-\frac{\big[\vec{b}+(1/2-\alpha)\vec{r}\big]^2}{2\mathcal{B}(x)}\right]\Bigg\}\,. \end{aligned} \quad (6)$$

The function $\mathcal{B}(x)$ reads [12]

$$\mathcal{B}(x) = B_{el}^{\bar{q}q}(x,r\to 0) - \frac{r_s^2}{8(1-e^{-r_s^2/R_0^2(x)})}\,, \quad (7)$$

where $r_s = \frac{Y}{\sqrt{Q^2+m_V^2}}$ is scanning radius, factor $Y\approx 6$ for charmonia and $R_0^2(x)$ controls the x dependence of saturation cross section. In this work, we employ the latest GBS model by Golec-Biernat and Sapeta including the Dokshitzer-Gribov-Lipatov-Altarelli-Parisi (DGLAP) evolution [17]. Here the saturation scale is related to the gluon density, $R_0^2(x,\mu^2) = 4/Q_s^2(x,\mu^2) = \sigma_0\,N_c/\big(\pi^2\,\alpha_s(\mu^2)\,x\,g(x,\mu^2)\big)$, where $\mu^2 = C/r^2+\mu_0^2$, Q_s^2 is the saturation scale, and the gluon distribution function $x\,g(x,\mu^2)$ is obtained as a solution of the DGLAP evolution equation with the form at the initial scale $Q_0^2 = 1$ GeV^2, $x\,g(x,Q_0^2) =$

$A_g\, x^{-\lambda_g}(1-x)^{5.6}$. Here $A_g = 1.07$, $\lambda_g = 0.11$, $\mu_0^2 = 1.74$ GeV^2, C= 0.27 and $\sigma_0 = 22.93$ mb. The quantity $B_{el}^{\bar{q}q}(x, r \to 0)$ refers to the elastic diffraction slope parametrized as [18, 12]

$$B(W,Q^2) = B_0 + 4\alpha'(0)\ln\Big(\frac{W}{W_0}\Big) - \Delta_V(Q^2)\,, \tag{8}$$

with parameters $B_0 = 4.4\,\mathrm{GeV}^{-2}$, $W_0 = 90$ GeV, $\alpha'(0) = 0.133\,\mathrm{GeV}^{-2}$ obtained from fit to combined H1 [19, 20] and ZEUS [21, 22] data. Parameter $\Delta_V(Q^2)$ for J/ψ has a phenomenological form

$$\Delta_{J/\psi}(Q^2) = B_1 \ln\Big(\frac{Q^2 + M_{J/\Psi}^2}{M_{J/\psi}^2}\Big)\,, \tag{9}$$

where $B_1 = 0.45$ GeV^{-2}. For ψ', due to the non-negligible influence of the nodal structure, the factor $\Delta_{J/\psi}(Q^2)$ is transformed into $\Delta_{\psi'}(W,Q^2)$ by adding a positive-valued term [18]

$$\Delta_{\psi'}(W,Q^2) = \Delta_{J/\psi}(Q^2) + c(W)\Big(1 - d(W)\ln\Big(\frac{Q^2 + M_{\psi'}^2}{M_{\psi'}^2}\Big)\Big)\,, \tag{10}$$

where $c(W) = 0.24\, -\, 0.08\ln\Big(\frac{W}{W_0}\Big)$ GeV^{-2}, $d(W) = 1.65\, +\, 0.3\ln\Big(\frac{W}{W_0}\Big)$.

We consider a small real part of the dipole-proton amplitude included via the following substitution

$$\mathrm{Im}\mathcal{A}^N_{\bar{Q}Q}(\vec{r}, x, \alpha, \vec{b}\,) \Rightarrow \mathrm{Im}\mathcal{A}^N_{\bar{Q}Q}(\vec{r}, x, \alpha, \vec{b}\,)\cdot\left(1 - i\,\frac{\pi\,\Lambda}{2}\right)\,, \qquad \Lambda = \frac{\partial\,\ln\,(\mathrm{Im}\mathcal{A}^N_{\bar{Q}Q}(\vec{r}, x, \alpha, \vec{b}\,))}{\partial\,\ln(1/x)}\,. \tag{11}$$

Next, we include also skewness correction [23] by multiplying the dipole-proton amplitude by a factor $R_S(\Lambda) = (2^{2\,\Lambda+3}/\sqrt{\pi}\,)\cdot\Gamma(\Lambda+5/2)/\Gamma(\Lambda+4)$. The gluon shadowing effect on nuclear targets is considered via correction factor $R_G(x, |\vec{b}+\vec{b_A}|)$ which reduces the partial dipole-proton amplitude at sufficiently large values of Bjorken x

$$\mathrm{Im}\mathcal{A}^N_{\bar{Q}Q}(\vec{r}, x, \alpha, \vec{b}\,) \Rightarrow \mathrm{Im}\mathcal{A}^N_{\bar{Q}Q}(\vec{r}, x, \alpha, \vec{b}\,)\cdot R_G(x, |\,\vec{b}_A + \vec{b}\,|)\cdot R_S(\Lambda)\,. \tag{12}$$

The factor $R_G(x, |\vec{b}+\vec{b_A}|)$ was calculated for the $Q\bar{Q}G$ Fock component of the photon using the Green's function formalism [24].

The evolution of $Q\bar{Q}$ pair in the nuclear medium with initial separation $\vec{r_1}$ at the point z_1 completed by the formation of the vector meson wave function at point $z_2 \to \infty$ with final separation $\vec{r_2}$ is described by the Green's function $G_{Q\bar{Q}}(z_2, \vec{r}_2; z_1, \vec{r}_1|\vec{b}_A)$ in Eq. (4) which satisfies the following Schrödinger equation

$$i\frac{d}{dz_2}\,G_{Q\bar{Q}}(z_2, \vec{r}_2; z_1, \vec{r}_1|\vec{b}_A) = \left[\frac{\eta^2 - \Delta_{r_2}}{2\,p\,\alpha\,(1-\alpha)} + V_{Q\bar{Q}}(z_2, \vec{r}_2, \alpha, \vec{b}_A)\right] G_{Q\bar{Q}}(z_2, \vec{r}_2; z_1, \vec{r}_1|\vec{b}_A)\,, \tag{13}$$

where p is the photon energy in the target rest frame, $\eta^2 = m_Q^2 + \alpha(1-\alpha)Q^2$, m_Q is the heavy quark mass, and the Laplacian Δ_{r_2} acts on the coordinate r_2. The real part of the complex LF potential $V_{Q\bar{Q}}(z_2, \vec{r}_2, \alpha)$ describes the interaction of Q and $\bar{Q}$ and the procedure how to obtain it from any realistic $Q\bar{Q}$ interaction potential in the rest frame was discussed in detail in Ref. [13]. The imaginary part of the LF potential is responsible for the absorption of $Q\bar{Q}$ pair in the medium and is of the form

$$\mathcal{I}m V_{Q\bar{Q}}(z_2, \vec{r}, \alpha, \vec{b}_A) = -\int d^2b'\,\mathcal{A}^N_{\bar{Q}Q}(\vec{r}, x, \alpha, \vec{b}\,')\,\rho_A(\vec{b}\,' + \vec{b}_A, z_2)\,. \tag{14}$$

Finally, the expression for the t-dependent differential cross section reads

$$\frac{d\sigma^{\gamma^* A\to VA}(x, Q^2, t = -q^2\,)}{dt} = \frac{1}{16\pi}\left(\Big|\mathcal{A}_T^{\gamma^* A\to VA}(x, Q^2, \vec{q}\,)\Big|^2 + \tilde{\varepsilon}\,\Big|\mathcal{A}_L^{\gamma^* A\to VA}(x, Q^2, \vec{q}\,)\Big|^2\right)\,, \tag{15}$$

where subscript T and L refer to transversely or longitudinally polarized amplitude, respectively, and photon polarization $\tilde{\varepsilon} = 0.99$.

3 Results

We study the momentum transfer dependence in coherent photo- and electroproduction of charmonia ($J/\psi, \psi'$) on a gold target employing the quarkonium wave function generated by the power-like (POW) $Q\bar{Q}$ interaction potential [25]. For the parameters of the dipole-proton partial amplitude, we adopted the recent model by Golec-Biernat and Sapeta [17], denoted as GBS, including the DGLAP evolution.

First, we compared our calculations of t-dependent differential cross sections for photo- and electroproduction of J/ψ and ψ' with available data. In Figure 1, we present the t-dependent cross section $d\sigma/dt$ as a function of photon energy W for several fixed values of t for photo- (left) and electroproduction (right) of J/ψ on a proton target. Our calculations are in good agreement with data from the H1 collaboration [19]. In the left panel of Figure 2, we present the t-integrated cross section as a function of W for photoproduction of ψ' on a proton target in good agreement with LHCb data [26]. The right panel of Figure 2 shows $d\sigma/dt$ as a function of t for photoproduction of J/ψ on lead at photon energy $W = 125$ GeV. The model calculations including gluon shadowing are in good agreement with ALICE data [27].

Next, in Figure 3 we present the calculations of t-dependent cross section as a function of photon energy W for photoproduction (left) and electroproduction (right) of J/ψ on a gold target for several fixed values of t. Solid lines were calculated with the Green's function approach including gluon shadowing and the dashed lines represent calculations within the Eikonal approximation. At low photon energies, below 100 GeV corresponding to the EIC kinematic region, we observe the onset of reduced coherence length effects, i.e. the difference between the dashed and solid lines. However, for photoproduction it starts to be visible at rather small energies around $W = 20$ GeV, i.e. at the lower limit of the future EIC experiment. In the case of coherent electroproduction of charmonia (see the right panel of Figure 3), the onset of reduced coherence length effect starts to be visible at higher photon energies, $W \leq 50$ GeV. It provides a better chance for experimental observation of this effect. At high photon energies, in the kinematic region relevant for LHeC, the plot demonstrates how the gluon shadowing phenomenon affects the energy behavior of the t-dependent cross section. We see that the monotonic rise of the cross section at $|t| = 0.001$ GeV^2 with energy is gradually changed to a non-monotonic dependence at higher values of momentum transfer t. For photoproduction and $|t| = 0.012$ GeV^2, we observe a maximum at $W \sim 200$ GeV. This non-monotonic dependence of the t-dependent cross section on energy may be a signature of the gluon saturation effect in coherent charmonium photoproduction. On the other hand, the decrease of the t-dependent cross section at high energies is much less pronounced in electroproduction (see the right panel of Figure 3), and thus the chance to observe the saturation effect is in this case significantly reduced. This is caused by the weaker leading twist correction corresponding to a weaker onset of non-linear QCD evolution in comparison with photoproduction. Similar behavior of t-dependent cross section is observed also in photo- and electroproduction of excited ψ' state (not shown in the figure).

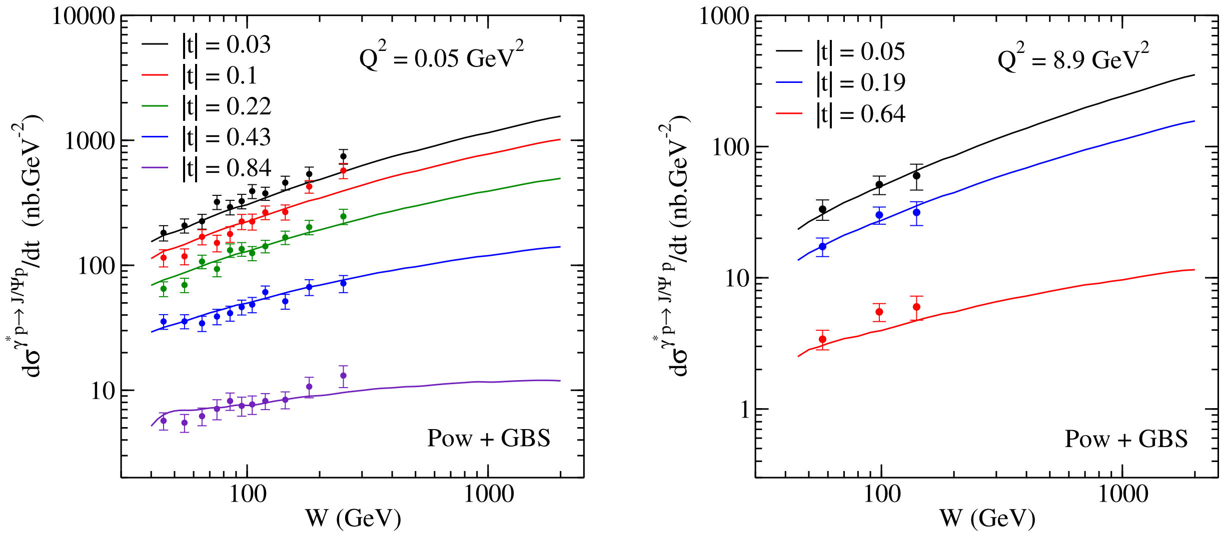

Figure 1 – Distributions $d\sigma^{\gamma(\gamma^*)p\to J/\psi p}(t)/dt$ at $Q^2 = 0.05$ GeV^2 (left) and at $Q^2 = 8.9$ GeV^2 (right) for production of J/ψ on proton target as a function of photon energy W for several fixed values of t vs data from the H1 collaboration [19]. Figure adopted from Ref. [2].

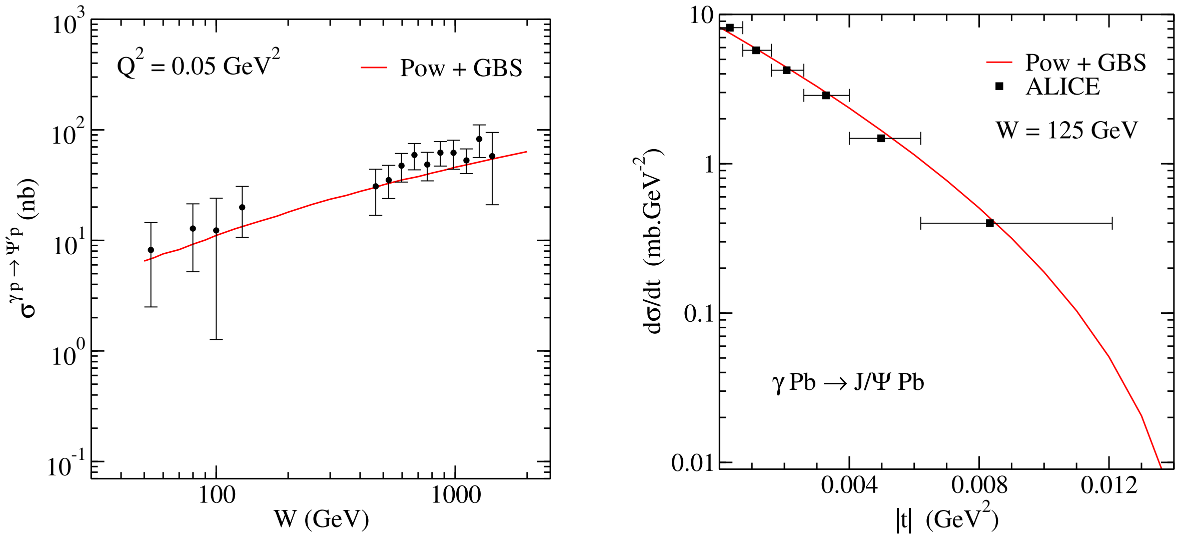

Figure 2 – t-integrated differential cross section (left) in the photoproduction of ψ' on a proton target compared with LHCb data [26]. The cross section $d\sigma(t)/dt$ (right) as a function of t for photoproduction of J/ψ on the lead target at photon energy W = 125 GeV ($\sqrt{s_{NN}}$ = 5.02 TeV), calculated including the gluon shadowing effects and compared with ALICE data [27]. Figure adopted from Ref. [2].

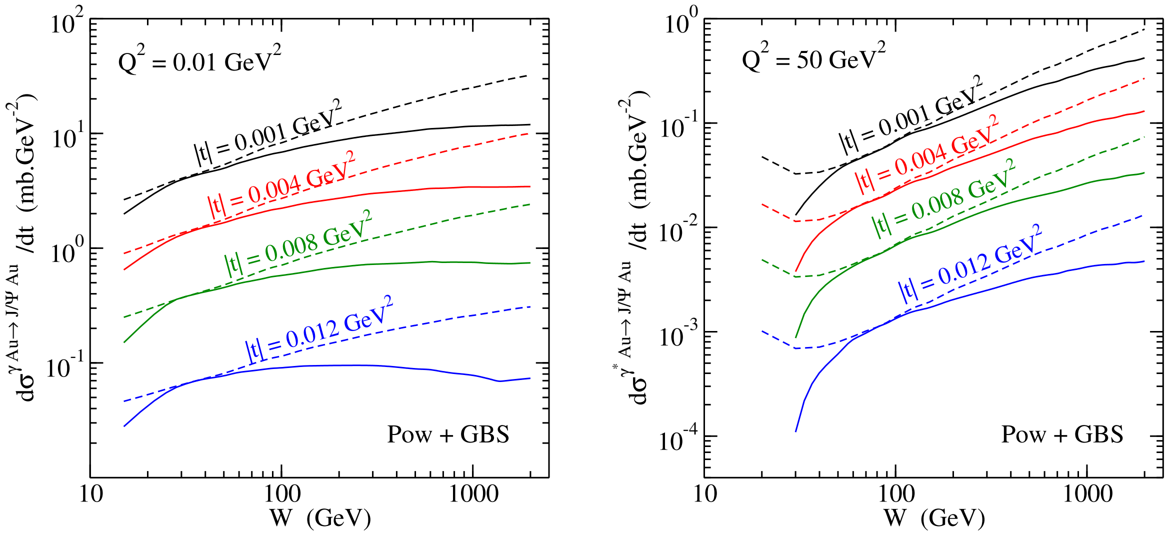

Figure 3 – Model predictions for the energy behavior of the t-dependent differential cross section $d\sigma/dt$ for coherent photoproduction (left) and electroproduction (right) of J/ψ on a gold target at several fixed values of $|t| = 0.001, 0.004, 0.008$ and 0.012 GeV^2, using the Green's function approach including gluon shadowing (solid lines) and with the Eikonal approximation without gluon shadowing (dashed lines). Figure adopted from Ref. [2].

The maximum for $|t| = 0.012$ GeV^2 in photoproduction of ψ' is shifted to larger values of photon energy $W \sim 500$ GeV.

4 Conclusions

We studied the transverse momentum transfer dependence of the differential cross section $d\sigma/dt$ in photo- and electroproduction of charmonia on a nuclear target using the color dipole approach based on the Green's function formalism. Such a formalism properly takes into account the reduced coherence length effects for the lowest $Q\bar{Q}$ Fock component of the photon at energies accessible by the future EIC experiment at BNL. Moreover, we also considered the contribution of photon fluctuations containing gluons to nuclear shadowing, which manifests itself at high photon energies corresponding to current LHC and future LHeC kinematical regions. It represents the leading twist correction due to the large, nearly scale-independent size of the $Q\bar{Q} - G$ dipoles. This size fluctuates during dipole propagation through the nucleus even at very high energies, because of divergent $d\alpha_g/\alpha_g$ behavior. For this reason, the corresponding calculations of gluon shadowing are based on the path-integral technique, which allows to include properly the lifetime also for multi-gluon photon components. Moreover, in contrast to the global data analyses, the leading twist shadowing correction contains also the dependence on the nuclear impact parameter b_A, which is crucial for evaluation of the t-dependent differential cross sections.

Our results, based on the GBS model with the DGLAP evolution for partial dipole-nucleon amplitude and POW potential for charmonium wave function, yield good agreement with available data on $d\sigma/dt$ on proton and lead targets. Model predictions for photo- and electroproduction of J/ψ on a gold target show the behavior of $d\sigma/dt$ for several fixed t values in a wide energy region, $10 < W \leq 2000$ GeV. At low energies, $W < 100$ GeV, the reduced quark shadowing effect resulting from a small coherence length for $Q\bar{Q}$ fluctuation, $l_c \lesssim R_A$, significantly decreases the differential cross section $d\sigma/dt$ in comparison with the standard Eikonal approximation, when $l_c \gg R_A$. At high LHC and LHeC energies, when $l_c^G \gg d \sim 2$ fm, the gluon shadowing becomes a dominant effect reducing significantly the results of calculations obtained within the Eikonal limit. Such an effect, corresponding to a non-linear QCD evolution, causes the non-monotonic behavior of $d\sigma/dt$, with a maximum, which is clearly visible for high value of $|t| = 0.012$ GeV^2 in photoproduction of J/ψ. This behavior may lead to a signature of possible gluon saturation and can be verified by the future LHeC experiments.

Acknowledgments

The work of J.N. was partially supported by the Slovak Funding Agency, Grant No. 2/0020/22. Computational resources were provided by the e-INFRA CZ project (ID:90254), supported by the Ministry of Education, Youth and Sports of the Czech Republic.

References

1. B. Z. Kopeliovich, M. Krelina, J. Nemchik and I. K. Potashnikova, Phys. Rev. D **105**, 054023 (2022), doi:10.1103/PhysRevD.105.054023
2. J. Nemchik and J. Óbertová, submitted to Phys. Rev. D (2025), arXiv:2507.01531 [hep-ph]
3. B. Z. Kopeliovich, A. Schäfer and A. V. Tarasov; Phys. Rev. D **62**, 054022 (2000), doi:10.1103/PhysRevD.62.054022
4. B. Z. Kopeliovich, J. Raufeisen and A. V. Tarasov, Phys. Rev. C **62**, 035204 (2000), doi:10.1103/PhysRevC.62.035204
5. A. Accardi *et al.*, Eur. Phys. J. A **52**, 268 (2016), doi:10.1140/epja/i2016-16268-9
6. P. Agostini *et al.* [LHeC and FCC-he Study Group], J. Phys. G **48**, 110501 (2021), doi:10.1088/1361-6471/abf3ba
7. I. Balitsky, Nucl. Phys. B **463**, 99 (1996), doi:10.1016/0550-3213(95)00638-9
8. Y. V. Kovchegov, Phys. Rev. D **60**, 034008 (1999), doi:10.1103/PhysRevD.60.034008
9. L. V. Gribov, E. M. Levin and M. G. Ryskin, Nucl. Phys. B **188**, 555 (1981), doi:10.1016/0550-3213(81)90007-9
10. L. V. Gribov, E. M. Levin and M. G. Ryskin, Phys. Rept. **100**, 1 (1983), doi:10.1016/0370-1573(83)90022-4
11. B. Z. Kopeliovich and B. G. Zakharov; Phys. Rev. D **44**, 3466 (1991), doi:10.1103/PhysRevD.44.3466
12. B. Z. Kopeliovich, M. Krelina and J. Nemchik, Phys. Rev. D **103**, 094027 (2021), doi:10.1103/PhysRevD.103.094027
13. J. Nemchik and J. Óbertová, Phys. Rev. D **110**, 054015 (2024), doi:10.1103/PhysRevD.110.054015
14. H. De Vries, C. W. De Jager and C. De Vries, Atom. Data Nucl. Data Tabl. **36**, 495 (1987), doi:10.1016/0092-640X(87)90013-1
15. M. V. Terentev, Sov. J. Nucl. Phys. **24**, 106 (1976) [Yad. Fiz. **24**, 207 (1976)].
16. H. J. Melosh, Phys. Rev. D **9**, 1095 (1974), doi:10.1103/PhysRevD.9.1095
17. K. Golec-Biernat and S. Sapeta, JHEP **03**, 102 (2018), doi:10.1007/JHEP03(2018)102
18. J. Cepila, J. Nemchik, M. Krelina and R. Pasechnik, Eur. Phys. J. C **79**, 495 (2019), doi:10.1140/epjc/s10052-019-7016-9
19. A. Aktas *et al.* [H1], Eur. Phys. J. C **46**, 585 (2006), doi:10.1140/epjc/s2006-02519-5
20. C. Alexa *et al.* [H1], Eur. Phys. J. C **73**, 2466 (2013), doi:10.1140/epjc/s10052-013-2466-y
21. J. Breitweg *et al.* [ZEUS], Z. Phys. C **75**, 215 (1997), doi:10.1007/s002880050464
22. S. Chekanov *et al.* [ZEUS], Eur. Phys. J. C **24**, 345 (2002), doi:10.1007/s10052-002-0953-7

23. A. G. Shuvaev, K. J. Golec-Biernat, A. D. Martin and M. G. Ryskin, Phys. Rev. D **60**, 014015 (1999), doi:10.1103/PhysRevD.60.014015
24. M. Krelina and J. Nemchik, Eur. Phys. J. Plus **135**, 444 (2020), doi:10.1140/epjp/s13360-020-00498-2
25. N. Barik and S. N. Jena, Phys. Lett. B **97**, 265 (1980), doi:10.1016/0370-2693(80)90598-5
26. R. Aaij *et al.* [LHCb], JHEP **10**, 167 (2018), doi:10.1007/JHEP10(2018)167
27. S. Acharya *et al.* [ALICE], Phys. Lett. B **817**, 136280 (2021), doi:10.1016/j.physletb.2021.136280